Micro and Nano Systems Letters

LETTER

Open Access

Improvement of fiber optic based localized surface plasmon resonance sensor by optical fiber surface etching and Au capping

Se-Woong Bae†, Hyeong-Min Kim†, Jae-Hyoung Park* and Seung-Ki Lee*

Abstract

Fiber optic based localized surface plasmon resonance (FO-LSPR) sensor is one of the biosensors that detects specific biomolecules and can detect the onset of disease. In this paper, we propose two methods to improve the signal to noise ratio (SNR) of the sensor, which is one of the main characteristics of the FO-LSPR sensor. The first method is to increase the intensity of the sensor by increasing the size of gold nanoparticle (Au NP) formed on the optical fiber surface by Au capping method. The second method is to form a structure that reduces the reflection by increasing the roughness of the surface by etching the surface of the optical fiber using the Au NP formed on the surface of the optical fiber as a mask. Increasing the roughness of the optical fiber surface can reduce the background signal of the sensor. The two methods mentioned above can increase the SNR of the sensor. When the SNR of the sensor is increased, the efficiency of the sensor is improved.

Keywords: Au nanoparticle, Localized surface plasmon resonance, Surface etching, Au capping, Signal-to-noise ratio

Introduction

Biosensor can detect specific biomolecules such as viruses, bacteria and antigens using various types of receptors [1, 2]. The characteristics of the biosensor required for detecting a specific biomolecule include fast detection time, high sensitivity, miniaturization, manufacturing cost, etc. When fabricating the biosensor based on nanotechnology, all of these characteristics can be satisfied. Typical measurement methods used in biosensors are ellipsometry, fluorescence, surface plasmon resonance (SPR), localized surface plasmon resonance (LSPR), surface-enhanced raman spectroscopy (SERS), etc. [3–12]. Using these measurement methods, sensor's intensity for biomolecules with various concentrations can be measured and the characteristics of the sensor such as measurement range, linearity, limit of detection (LOD), signal to noise ratio (SNR) etc. for the sensor can be confirmed.

Among various biomolecules that cause disease, there are specific biomolecules that can become diseased even at very low concentrations in the blood. In order to measure such a biomolecule, the sensor must be able to measure biomolecules at a very low concentration. Therefore, the SNR of the sensor is one of the important characteristics of the sensor. It is important to lower the sensor's noise or improve the sensor intensity to increase the SNR.

In the previous paper, it showed two performance improvements with Au capping process that can control the size of gold nanoparticle (Au NP) [13]. First, the sensitivity of the sensor was improved by increasing the size of Au NPs. Second, the binding force between the optical fiber surface and the nanoparticles caused by bigger Au NP improved the stability of the sensor. In this paper, we fabricate a fiber optic based LSPR sensor (FO-LSPR) and propose two methods to improve the SNR of the sensor. The first method is to increase the LSPR intensity of the sensor by increasing the size of Au NP using Au capping. As shown in Fig. 1a, the FO-LSPR sensor is used as a sensor by immobilization Au NPs to the surface of

*Correspondence: parkjae@dankook.ac.kr; skilee@dankook.ac.kr
†Se-Woong Bae and Hyeong-Min Kim contributed equally to this work
Department of Electronics and Electrical Engineering, Dankook University, Yongin 16890, South Korea

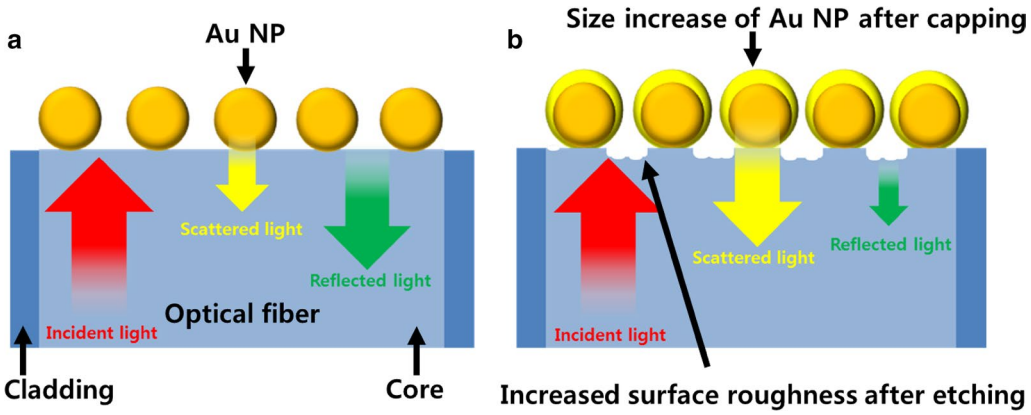

Fig. 1 Schematic diagram of the FO-LSPR sensor **a** without and **b** with Au capping and etching process

the optical fiber cross-section. In previous study, it was confirmed that the size of Au NP could be increased additionally from several nm to several tens nm by Au capping [13]. The second method is to increase the roughness of the optical fiber surface which is not covered with Au NPs by an etching process using Au NPs formed on the optical fiber surface as a mask. As shown in Fig. 1b, when the size of Au NP is increased additionally by the first method, the amount of the scattered light is increased [13, 14]. The roughness of the optical fiber surface is increased due to the second method so that the reflected light which is the background signal of the sensor's intensity from the surface of the optical fiber is reduced [15]. As a result, the SNR of the FO-LSPR sensor is increased.

The FO-LSPR sensor is fabricated and modified using the above two methods. Through the measurement of the refractive indices (RI) using the fabricated sensor, we verify experimentally the increase of the intensity by the Au capping and the decrease of the background signal by the reduced reflection on the optical fiber surface. Also, the SNRs of the fabricated sensor for fine variation of the refractive index are measured and compared according to the change of the time of Au capping and etching.

Fabrication of FO-LSPR sensor

Multimode optical fiber (FG105LCA, Thorlabs) was used to fabricate the FO-LSPR sensor. The core diameter of the optical fiber was 105 μm and the diameter of the cladding was 125 μm. The polymer on the surface of the optical fiber was removed and the optical fiber was cut using an optical fiber cleaver (S326A, Fitel).

The method of manufacturing the FO-LSPR sensor consisted of three steps. First, the optical fiber was immersed in a piranha solution which was mixed with sulfuric acid (H_2SO_4, 95%, Daejung Chemicals) and hydrogen peroxide (H_2O_2, 34.5%, Samchun Chemical) in a volume ratio of 4:1 for 20 min. On the surface of the optical fiber, a hydroxy group (–OH) was formed by the piranha solution. Second, the optical fiber containing –OH was immersed in a solution of 5% (v/v) 3-(ethoxydimethylsilyl)-propylamine (APMES, 97%, Sigma Aldrich) for 90 min. After 90 min, a self-assembled monolayer (SAM) with amine groups on the optical fiber surface was formed. Third, the Au NPs were electrostatically fixed to the optical fiber surface by immersion the amine-formed optical fiber in a colloidal gold solution for 60 min [16–18]. Figure 2a is a SEM image of the Au NPs which were fabricated on the optical fiber surface by this method. The average diameter of Au NPs was measured to be about 49.5 ± 4.1 nm.

Increasing the intensity of the FO-LSPR sensor was done by increasing the size of Au NP by Au capping. The Au capping was proceeded in two steps. First, The Au NPs which were immobilized on the optical fiber surface were reacted with 0.5 mM an aqueous solution of 1% sodium citrate dehydrate ($C_6H_5Na_3O_7 \cdot 2H_2O$, 99%, Daejung Chemicals). After this, when the Au NPs were reacted with 1 mM of chloride trihydrate ($HAuCl_4 \cdot 3H_2O$, 99%, Sigma Aldrich), the size of Au NP was increased with the reduction of gold ions. In previous study [13], the size of Au NP was increased by 3.3 nm on average for 30 min in proportion to the time of reaction with $HAuCl_4$ solution. The Au NP was increased additionally up to 20 nm after 180 min of reaction. Figure 2b is a SEM image of the Au NPs on the optical fiber surface after Au capping. It shows that the size of Au NP is larger than that of Fig. 2a. As a result, the size of Au NP is increased as the injection time of chloride trihydrate solution increases.

Equation (1) based on the Mie theory, which is well known in the field of plasmonics, is an equation for

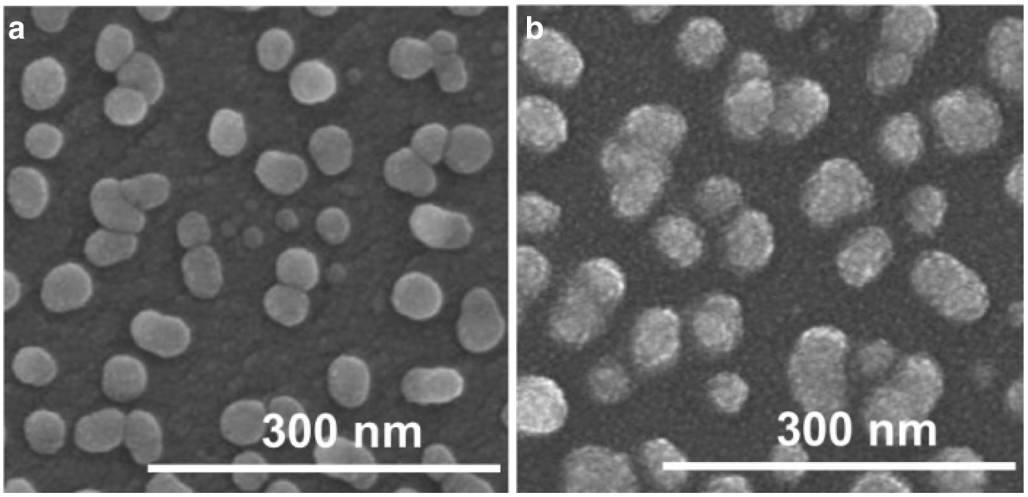

Fig. 2 The SEM images of Au NPs on the surface of the optical fiber **a** before and **b** after Au capping

the phenomenon that the amount of scattered light increases as the bigger Au NP size.

$$\sigma_{scatt} = -\left(\frac{128\pi^5}{3\lambda^4}\right)R^5\left[\frac{m^2-1}{m^2+2}\right]^2 \quad (1)$$

σ_{scatt} is the scattering cross-section area. As σ_{scatt} increases, the amount of scattered light collected from the optical fiber increases. λ is the wavelength of light which is incident to the Au NP, R is the radius of Au NP immobilized on the surface of the optical fiber, m is the ratio between the refractive index of the Au NP and the refractive index of the surrounding medium [19]. As expressed in Eq. (1), if λ and m have the fixed value, level of σ_{scatt} is dominantly influenced by the increase in the size of Au NP when the Au NP size (R) grows. As a result, the amount of collected light to the optical fiber through scattering from the Au NPs is increased due to the Au capping process. In this paper, we confirmed the increase of diameter about 14 nm on the average through the reaction for 2 h.

To form a structure with decreased background signal by roughening the optical fiber surface, reactive ion etching (RIE) was performed using the Au NPs as a mask (RIE 80 plus, Oxford instrument). As a result, the optical fiber surface not covered with the Au NP was roughened and the reflection from the surface was decreased.

The relationship between the surface roughness and the reflected light on the optical fiber surface which is not occupied by the Au NPs is shown in Eq. (2).

$$R_s = R_0\exp\left[-4(\pi\sigma)^2/\lambda^2\right] \quad (2)$$

R_s is the reflectance according to the surface roughness, R_0 is the reflectance of the smooth optical fiber surface, σ is the root mean square of the roughness (R_{rms}), and λ is the wavelength of the incident light [15]. In Eq. (2), R_0 and λ are same in all experiments. Therefore, R_s is dominantly influenced by σ that increases with etching time. As a result, when the surface of the optical fiber becomes rough due to the RIE etching process, the background signal decreases because the light which is reflected from the optical fiber surface except for the portion occupied by Au NPs is lowered.

Using the first fabrication method, the amount of the scattered light which is the output intensity of the sensor generated from the Au NPs was increased. Through the second fabrication method, the reflected light from the optical fiber surface, which is the background noise of the sensor intensity, was decreased. These fabrication methods can improve the performance of the fabricated FO-LSPR sensor.

Measurement system of FO-LSPR sensor

The measurement system for the experiment using the fabricated FO-LSPR sensor is shown in Fig. 3. The FO-LSPR sensor is placed in the reaction chamber inside the microfluidic channel to minimize the contact time between the sensor and external air, and four inlet ports and one outlet port are made to facilitate the exchange of the measurement solution [20]. The measurement system of the FO-LSPR sensor which is combined with the microfluidic channel consists of the light source, 2×1 coupler and spectrometer. There are three optical transmission paths in the 2×1 coupler. The first part is connected to the light source to transmit the light from the

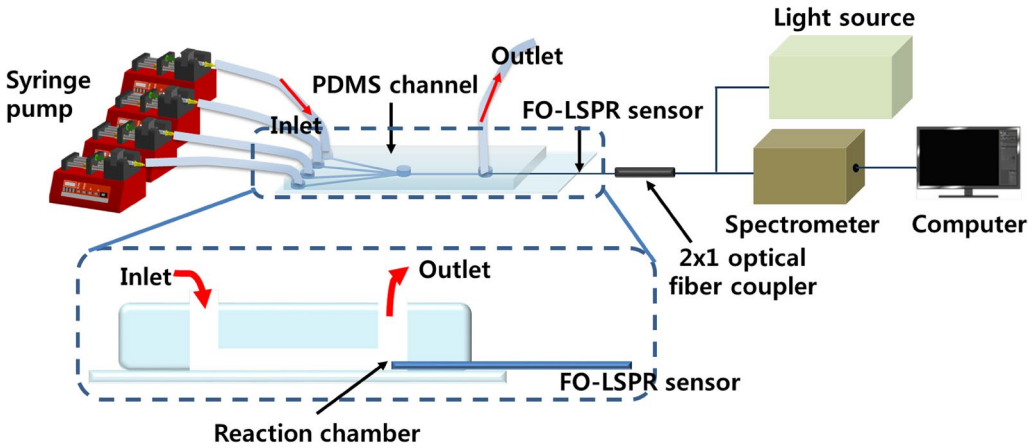

Fig. 3 Schematic diagram of the FO-LSPR sensor measurement system

light source. The second part is connected to the FO-LSPR sensor to transmit light to the sensor. The third part is connected to the spectrometer to receive scattered light from the sensor. Using the 2×1 coupler, the light which is scattered by the Au NPs is transmitted to the spectrometer to measure the signal.

Measurement of refractive indices using FO-LSPR sensor

The LSPR signal according to the refractive index was measured by increasing the refractive index of the solution from 1.33 to 1.38 by 0.01 using the FO-LSPR sensor. The FO-LSPR sensors were fabricated with various Au capping time and etching time. The Au capping time was changed to 0, 1 and 2 h to increase the size of Au NP, and the etching time was changed to 0, 5, 10 and 15 s to increase the surface roughness of the optical fiber. Measured LSPR signals varying refractive indices with the change of the etching time and the Au capping time are shown in Fig. 4. In Fig. 4, (a) is a graph showing the LSPR signal of RI = 1.33, (b) RI = 1.35 and (c) RI = 1.37, respectively. As the etching time is increased, the roughness of the optical fiber surface is increased, so the background signal is decreased. As the Au capping time is increased, the size of Au NP is increased, so the LSPR signal is increased. As a result, the normalized intensity in Fig. 4 which was obtained by dividing the output intensity of the sensor by the background noise has increased as the increase of etching time and Au capping time.

Measurement of background signal using FO-LSPR sensor

Using the Au NPs as a mask, the RIE etching was performed on the surface of the optical fiber which was not occupied by Au NPs for 5, 10, and 15 s, respectively, to fabricate the sensor. The Au NPs were removed to measure the roughness of the optical fiber surface which is fabricated by the RIE etching process. Figure 5 shows the measurement of the optical fiber surface from which Au NPs were removed using a 3D surface profiler. Figure 5, (a) is an image of 0 s etched optical fiber surface, (b) is 5 s etched optical fiber, (c) is 10 s etched optical fiber, and (d)

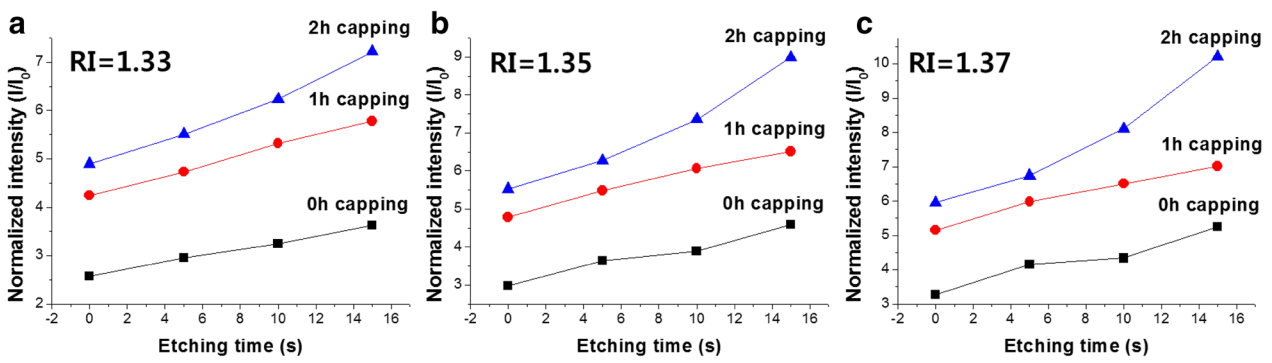

Fig. 4 LSPR signal change with Au capping time and etching time **a** RI = 1.33, **b** RI = 1.35, **c** RI = 1.37

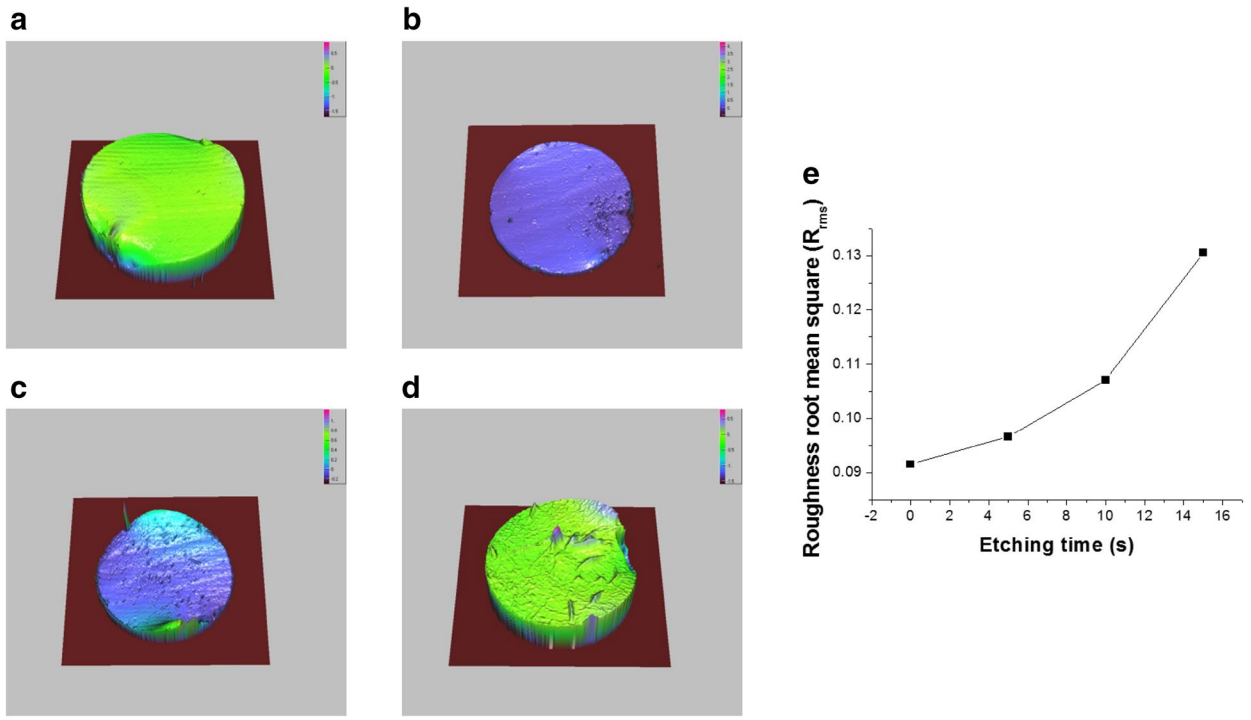

Fig. 5 Optical fiber surface image measured with 3D surface profiler **a** 0 s etching, **b** 5 s etching, **c** 10 s etching, **d** 15 s etching, respectively, and **e** roughness root mean square of the surface of optical fiber with etching time

is 15 s etched optical fiber, respectively. Figure 5e shows the relationship between the calculated R_{rms} of the surface of the optical fiber and the etching time.R_{rms} was calculated using Eq. (3) [21].

$$R_{rms} = \sqrt{\frac{1}{n}\sum_{i=1}^{n} y_i^2} \tag{3}$$

y_i is the height from the mean line, n is the number of intersections of the profile at the mean line. The R_{rms} was obtained from the measurement area (30 μm × 30 μm) of five zones each of the top, bottom, left, right, and center of the optical fiber surface.

Using Au NPs as a mask, RIE etching was performed on the optical fiber area which was not covered with the Au NPs. As a result, the R_{rms} of the surface of the optical fiber increased in proportion to the etching time.

The background signal of the sensor was directly measured to confirm that the surface of the FO-LSPR sensor was roughened by etching to reduce the reflection. The background signal of the FO-LSPR sensor means the output intensity of the sensor in the absence of Au NPs. After removing the Au NPs of the sensors of which surfaces were etched for 5, 10 and 15 s respectively, we measured the background signal according to the refractive indices change by increasing refractive index of the solution from 1.33 to 1.38 by 0.01. Measured results show that the background signal has decreased as the etching progressed as shown in Fig. 6. As a result, when etching was performed using the Au NPs as a mask, the structure for reducing reflection on the optical fiber surface was formed. Also, since the surface roughness was increased with the etching time,

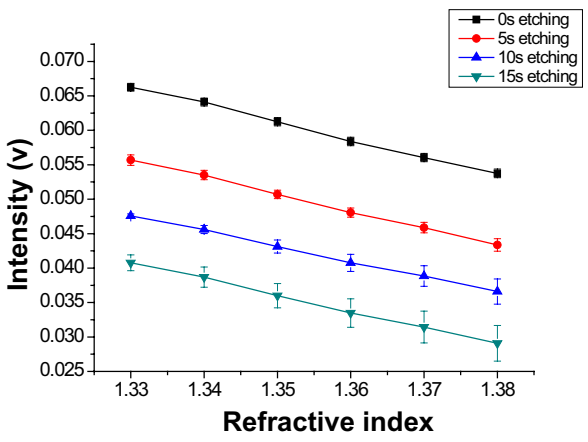

Fig. 6 Change of background noise due to refractive indices change

the amount of reflected light was decreased with the increase of the etching time.

Measurement of change in fine refractive index using FO-LSPR sensor

Since the background signal was decreased through the etching process on the FO-LSPR sensor, the noise generated during the measurement using the FO-LSPR sensor could be decreased. The SNR increases as the noise decreases, so that the fine change of refractive index can be measured. The sensors used in this experiment were four types of sensors with different Au capping and etching time, one for 0 and 2 h for Au capping time, and one for 0 and 15 s for etching. The experimental method was to increase the refractive index of solution from 1.333 to 1.334 by 0.001 and to measure the intensity of the sensor. Figure 7 shows the change of the sensor intensity when the refractive index changes by 0.001. The Au capping time and etching time were set to 0 h, 0 s (a), 0 h, 15 s (b), 2 h, 0 s (c), and 2 h, 15 s (d), respectively.

From the above measurement, the SNR can be defined as follow.

$$\mathrm{SNR} = \Delta \mathrm{I} \,/\mathrm{Background\ noise} \tag{4}$$

In Eq. (4), SNR is defined as dividing the change of the sensor intensity due to the refractive index change by the average value of the noise at each refractive index. Table 1 shows the SNR measurement results for the four cases of Fig. 6 using Eq. (4). As the Au capping time was increased from 0 h to 2 h, the SNR of the sensor with the etching time of 0 s was increased by 1.89 times from 1.45 to 2.74, and the sensor with the

Table 1 SNR of the FO-LSPR sensor for different Au capping time and etching time

SNR	Au capping time (h)	
Etching time (s)	0	2
0	1.45	2.74
15	8.45	15.39

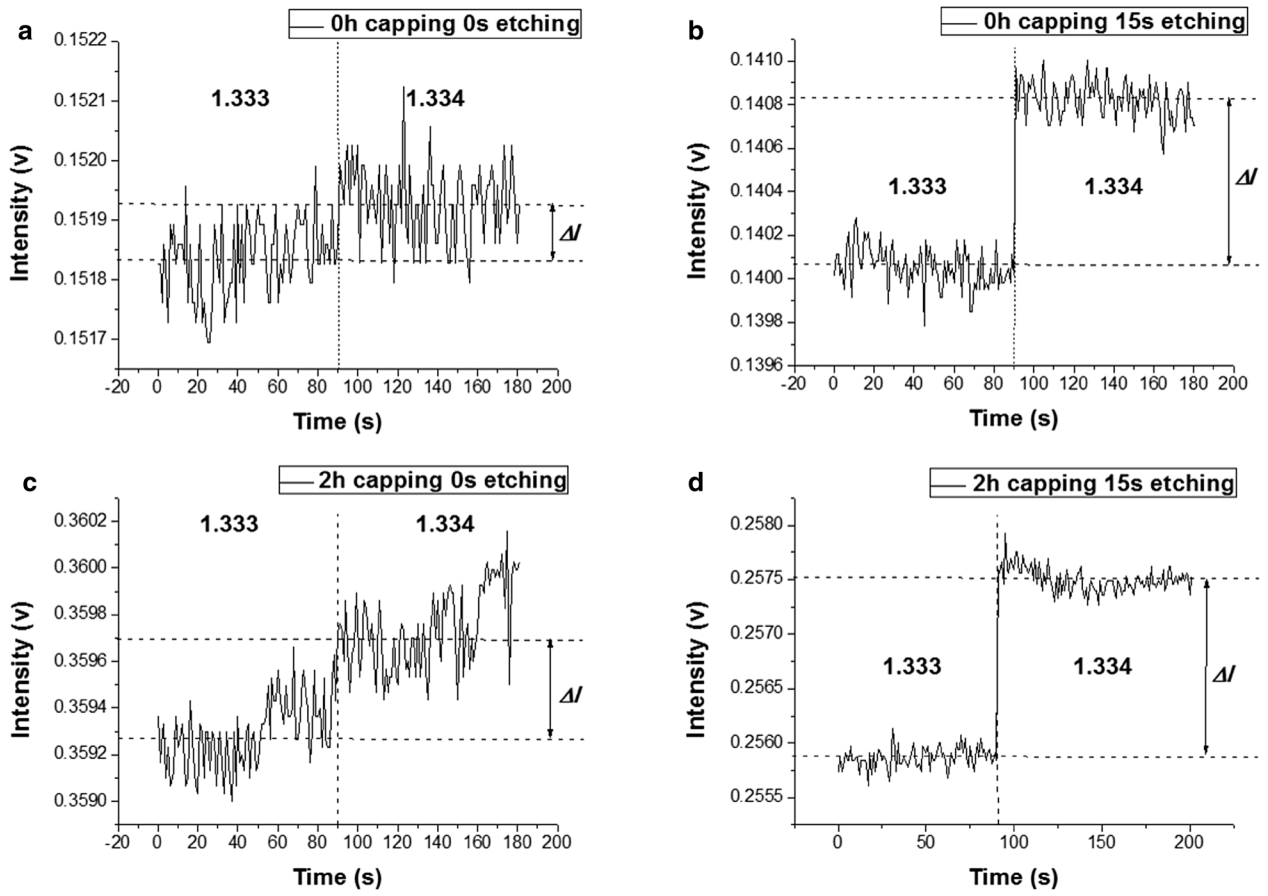

Fig. 7 Measurement of fine change of refractive index using FO-LSPR sensor with **a** 0 h Au capping and 0 s etching, **b** 0 h Au capping and 15 s etching, **c** 2 h Au capping and 0 s etching, and **d** 2 h Au capping and 15 s etching, respectively

etching time of 15 s was increased by 1.82 times from 8.45 to 15.39. As the etching time was increased from 0 s to 15 s, the SNR of the sensor with the Au capping time of 0 h was increased by 5.83 times f$_t$om 1.45 to 8.45, and the sensor with the Au capping time of 2 h was increased by 5.62 times from 2.74 to 15.39. The SNR of the sensor with the Au capping time of 2 h and the etching time of 15 s was increased by 10.61 times from 1.45 to 15.39 comparing with the sensor without Au capping and etching.

As a result, the two methods which were proposed to increase the SNR of the sensor could increase the SNR. Especially, increasing the roughness of the optical fiber surface through the etching process has more effect on increasing the SNR, and simultaneous application of both methods is more effective.

Conclusion

We increased the sensor intensity by increasing the size of Au NP using Au capping method and decreased the sensor background signal by increasing the roughness of optical fiber surface by etching process using the Au NP as a mask. From the measurement results using the fabricated FO-LSPR sensor, it was verified that the SNR of the sensor was increased with the increase of the Au capping time and the etching time. The proposed method can improve the SNR, one of the important characteristics of the sensor, so it is expected that it can be applied to accurate diagnosis of diseases through measurement of very low concentration of biomolecules present in the blood.

Abbreviations

LSPR: localized surface plasmon resonance; SNR: signal to noise ratio; Au NP: gold nanoparticle; FO-LSPR: fiber optic based localized surface plasmon resonance; RI: refractive index; RIE: reactive ion etching; R_{rms}: root mean square of the roughness.

Acknowledgements

Not applicable.

Authors' contributions

SKL, JHP devised the idea and supervised the project. SWB, HMK, JHP, and SKL discussed the design and experimental setup. HMK and SWB performed the experiment using the FO-LSPR sensor. SKL, HMK and SWB drafted the manuscript. All authors read and approved the final manuscript.

Funding

This work was supported by the National Research Foundation of Korea (NRF) Grant funded by the Korea government (MSIT) (No. NRF-2018R1A2B6001361).

Availability of data and materials

Not applicable

Competing interests

The authors declare that they have no competing interests.

Received: 6 June 2019 Accepted: 10 October 2019
Published online: 16 October 2019

References

1. Malhotra BD, Singhal R, Chaubey A, Sharma SK, Kumar A (2005) Recent trends in biosensors. Curr Appl Phys 5(2):92–97
2. Vo-Dinh T, Cullum B (2000) Biosensors and biochips: advances in biological and medical diagnostics. Fresenius'J Analyt Chem 336(6):540–551
3. Sarkar P, Turner APF (1999) Application of dual-step potential on single screen-printed modified xarbon paste electrodes for detection of amino acids and proteins. Fresenius'J Analyt Chem 364(1):154–159
4. Thevenot DR, Toth K, Durst RA, Wilson GS (2001) Electrochemical biosensors: recommended definitions and classification. Bioses Bioelectron 16(1):121–131
5. Feijter JAD, Benjamins J, Veer FA (1978) Ellipsometry as a tool to study the adsorption behavior of synthetic and biopolymers at the air–water interface. Biopolymers 17(7):1759–1772
6. Sciacca B, Monro TM (2014) Dip biosensor based on localized surface plasmon resonance at the tip of an optical fiber. Langmuir 30(3):946–954
7. Mayer KM, Hafner JH (2011) Localized surface plasmon resonance sensors. Chem Rev 111(6):3828–3857
8. Knez K, Janssen KPF, Spasic D, Declerck P, Vanysacker L, Denis C, Tran DT, Lammertyn J (2013) Spherical nucleic acid enhanced FO-SPR DNA melting for detection of mutations in legionella pneumophila. Anal Chem 85(3):1734–1742
9. Jeong HH, Lee SK, Park JH, Erdene N, Jeong DH (2011) Fabrication of fiber-optic localized surface plasmon resonance sensor and its application to detect antibody-antigen reaction of interferon-gamma. Opt Eng. 50(12):124405. https://doi.org/10.1117/1.3662418
10. Tu H, Sun T, Grattan KT (2013) SPR-based optical fiber sensors using gold-silver alloy particles as the active sensing material. IEEE Sens J 13(6):2192–2199
11. Yola ML, Atar N, Eren T (2014) Determination of amikacin in human plasma by molecular imprinted SPR nanosensor. Sens Actuators B: Chem 198:70–76
12. Atar N, Eren T, Yola ML, Wang S (2015) A sensitive molecular imprinted surface plasmon resonance nanosensor for selective determination of trace triclosan in wastewater. Sens Actuators B: Chem 216:638–644
13. Kim HM, Jeong DH, Lee HY, Park JH, Lee SK (2019) Improved stability of gold nanoparticles on the optical fiber and their application to refractive index sensor based on localized surface plasmon resonance. Opt Laser Technol 114:171–178
14. Tu MH, Sun T, Grattan KTV (2012) Optimization of gold-nano particle-based optical fiber surface plasmon resonance (SPR)-based sensors. Sens Actuators B: Chem 164:43–53
15. Bennett HE, Porteus JO (1961) Relation between surface roughness and specular reflectance at normal incidence. J Opt Soc Am 51:123–129
16. Chen J, Shi S, Su R, Qi W, Huang R, Wang M, Wang L, He Z (2015) Optimization and application of reflective LSPR optical fiber biosensors based on silver nanoparticles. Sensors 15(6):12205–12217
17. Jeong HH, Erdene N, Park JH, Jeong DH, Lee SK (2012) Analysis of fiber-optic localized surface plasmon resonance sensor by controlling formation of gold nanoparticles and its bio-application. J Nanosci Nanotechnol 12(10):7815–7821
18. Nayak JK, Parhi P, Jha R (2015) Graphene oxide encapsulated gold nanoparticle based stable fiber optic sucrose sensor. Sens Actuators B: Chem 221:835–841
19. van Dijk MA, Tchebotareva AL, Orrit M, Berciaud S, Lasne D, Cognet L, Lounis B (2006) Absorption and scattering microscopy of single metal nanoparticles. Phys Chem Chem Phys 8(30):3486–3495
20. Uh MH, Kim JS, Park JH, Jeong DH, Lee HY, Lee SM, Lee SK (2017) Fabrication of localized surface plasmon resonance sensor based on optical fiber and micro fluidic channel. J Nanosci Nanotechnol 17(2):1083–1091
21. Gadelmawla ES, Koura MM, Maksoud TMA, Elewa IM, Soliman HH (2002) Roughness parameters. J Mater Process Technol 123:133–145

Publisher's Note